A subset of viruses thrives following microbial resuscitation during rewetting of a seasonally dry California grassland soil

Alexa M. Nicolas[1], Ella T. Sieradzki[2*], Jennifer Pett-Ridge[3, 4], Jillian F. Banfield[2,5,6], Michiko E. Taga[1], Mary K. Firestone[2,6], Steven J. Blazewicz[3*]

[1]Plant & Microbial Biology Department, University of California, Berkeley, CA, USA

[2]Environmental Science, Policy & Management Department, University of California, Berkeley, CA, USA

[3]Physical and Life Sciences Directorate, Lawrence Livermore National Laboratory, Livermore, CA, USA

[4]University of California Merced, Life & Environmental Sciences Department, Merced, CA, USA

[5]Earth and Planetary Sciences, University of California, Berkeley, CA, USA

[6]Lawrence Berkeley National Laboratory, Berkeley, California, CA, USA

[*]Corresponding author email: blazewicz1@llnl.gov or ella.shir@gmail.com

ABSTRACT

Viruses are abundant, ubiquitous members of soil communities that kill microbial cells, but how they respond to perturbation of soil ecosystems is essentially unknown. Here, we investigated lineage-specific virus-host dynamics in grassland soil following “wet-up”, when resident microbes are both resuscitated and lysed after a prolonged dry period. Quantitative isotope tracing, time-resolved metagenomics and viromic analyses indicated that dry soil held a diverse but low biomass reservoir of virions, of which only a subset thrived following wet-up. Viral richness decreased by 50% within 24 h post wet-up, while viral biomass increased four-fold within one week. Counter to recent hypotheses suggesting temperate viruses predominate in soil, our evidence indicates that wet-up is dominated by viruses in lytic cycles. We estimate that viruses drive a measurable and continuous rate of cell lysis, with up to 46% of microbial death driven by viral lysis one week following wet-up. Thus, viruses contribute to turnover of soil microbial biomass and the widely reported CO_2 efflux following wet-up of seasonally dry soils.

INTRODUCTION

Soil viruses are abundant and ubiquitous – a gram of soil can hold more than 10^9 viral-like particles (VLPs)[1,2] and recent studies illustrate their immense taxonomic diversity and potential functions[3,4]. While metagenomic studies hint at many possible functions for soil viruses[5–7], much remains unknown about their quantitative effect on soil microbiome turnover and ecology, especially in response to a perturbation. In marine systems, viruses are critically important to ecosystem biogeochemistry, killing upwards of ~40% of bacteria daily and redistributing up to 55% of bacterial carbon via the 'viral shunt'[8–10]. This vast impact largely occurs through targeted predation shaping microbial community composition and via expression of viral-encoded metabolisms[8,11–13]. However, in soils, viral-focused 'omic methods (viromics) represent recent developments[14,15] and viral contributions to soil organic matter turnover or microbial mortality have yet to be quantified[16].

Arid and semi-arid soils cover over 40% of the Earth's terrestrial surface and support more than one third of the world's population[17]. Many of these systems experience prolonged periods of water-deficit, after which, the first rainfall, 'wet-up', serves as a pivotal moment which resuscitates soil microbial activity and causes a rapid efflux of mineralized CO_2 (the "Birch Effect"[18]) that contributes disproportionately to annual carbon turnover[19,20]. This CO_2 pulse has been linked to the rapid growth and death of soil microorganisms[19,21,22], but the mechanisms driving these disturbance-induced successional patterns are unclear. Given observed differential mortality for microbial phyla after rewetting (e.g. Actinobacteria and Proteobacteria)[19,23] we hypothesized that soil viruses may be induced by rewetting and act both as a top-down control on microbial community assembly and a proximal driver behind the huge wet-up release of mineralized carbon.

55 The ecological triggers of lysogenic to lytic transitions is not well understood for temperate soil
56 viruses[24,25], but may be stimulated by stress events or shifts in environmental conditions such as
57 wet-up. Lysogenic viral populations can be maintained in soil bacterial genomes as
58 prophages[24,26]. In culture, these prophages often encode an integrase gene that enables phage
59 recombination into the host chromosome[27,28]; upon certain cues, they may excise from host
60 chromosomes and enter a lytic cycle, ultimately lysing their host cell. Induction of
61 prophages can occur due to population stochasticity, external stresses that cause DNA
62 damage, or through quorum sensing pathways[29,30]. In certain marine systems, temperate
63 phages dominate and lysogenic to lytic transitions have been linked to increased bacterial
64 abundance[31], with more integrase-encoding phages found in locations with higher
65 environmental stresses[32]. Given the unique attributes of the soil environment – extraordinary
66 spatial heterogeneity, lack of mixing, microniches of low nutrient availability[33] – some
67 hypothesize that lysogeny may be a predominant lifestyle of soil phages[2,6,26,30,34,35]. Previous
68 studies have shown that soil moisture modulates soil viral counts, composition, and activity[36,37],
69 and in arid and Mediterranean systems, soil microbes have substantially reduced activity and
70 replication during the summer dry-down[19,21,38,39], possibly favoring lysogeny as a mechanism to
71 persist. Thus, the burst of microbial growth that occurs after soil rewetting may suggest wet-up
72 too serves as an environmental trigger of viruses that had persisted through the summer-dry
73 down as prophages.
74
75 Here, we combined time-resolved viromics and quantitative stable isotope probing (qSIP)-
76 informed metagenomics[40,41] to follow dynamics of free viruses, VLPs, and those actively
77 infecting host cells, respectively. We used these data to understand lineage-specific viral-host
78 temporal patterns following rewetting, and how viruses restructure the soil microbiome and
79 contribute to cell death and carbon mineralization. In arid soils, abundant extracellular DNA and
80 dormant cells can mask active microbial populations[42–44], since up to 75% of cells may be

81 inactive at any given time in soil[45]. However, qSIP allowed us to directly identify active microbes
82 by tracing a stable isotope (^{18}O via $H_2{}^{18}O$) into the DNA of microbes and viruses actively
83 replicating in response to rewetting[23,46,47]. Measuring the subsequent shift in DNA density[48]
84 allowed us to calculate the growth and mortality rates of host microbes, and quantify viral
85 contribution to microbial turnover. We also addressed the question of whether rewetting serves
86 as a major inducer of prophages. This work builds on our previous efforts to link taxon-specific
87 population dynamics with rainfall-induced carbon fluxes[21,23].
88
89 **RESULTS**
90
91 *Viral Succession*
92
93 We established the set of metagenome assembled genomes (MAGs) and viral operational
94 taxonomic units (vOTUs) to define the soil microbiome following wet-up from 234 metagenomes
95 over five timepoints and 18 viromes over six timepoints (each in triplicate) generated from
96 California grassland soil collected at the end of the dry season (see Methods and our paired
97 study[49]). We combined these newly resolved MAGs with MAGs from a previous study at our
98 field site which sampled soil during the previous winter[40]. In total, we resolved 542 dereplicated
99 MAGs: 503 from total soil metagenomes comprised of diverse soil bacteria and archaea; and 39
100 from small size-fraction metagenomes[50], i.e., viral-enriched metagenomes or viromes which
101 include genomes from ultrasmall cells such as those of candidate phyla radiation (CPR)
102 bacteria. This study detected 26,368 dereplicated vOTUs from viromes (26,139) and
103 metagenomes (229) (Figure 1). We consider vOTUs detected in viromes to be extracellularized
104 VLPs, which are distinct from vOTUs detected in metagenomes where analysis cannot
105 differentiate between intracellular and extracellular viral populations (Supplementary Table 1).
106 Prior to rewetting, our microbial community was dominated by Actinobacteria and

107 Proteobacteria[49]. Similar to previous work[20,23], Proteobacteria were highly active throughout wet-
108 up and responded early to rewetting and Actinobacteria were also a top-responding lineage to
109 wet-up, but showed less overall activity despite their higher abundance (see Sieradzki et al.,
110 2022[49] for more details on the microbial and functional response to rewetting).
111
112 To visualize the spatial and temporal succession of microbial and viral populations, we
113 calculated ordinations based on the Bray-Curtis dissimilarity of relative abundance of MAGs
114 (Figure 2A left) and vOTUs (Figure 2A right). The first two principal components of MAG
115 abundances revealed that succession of potential hosts was most pronounced over time
116 (52.54% variance explained) with a minor spatial component and explained in total over 70% of
117 the variability. On the contrary, abundances of viruses had a significant spatial component. The
118 first two principal components of vOTUs represented a smaller variance compared to potential
119 hosts (35.6%). Overall, viruses showed more spatial heterogeneity than their hosts – most
120 viruses were only present in a single of three replicate microcosms whereas hosts (MAGs)
121 showed the reverse trend (Supplementary Figure 1A).
122
123 Following rewetting, we found that viral richness significantly decreases, while viral biomass
124 significantly increases. Early time points showed higher richness of vOTUs, but with lower
125 abundances per vOTU (Figure 2B, Supplementary Figure 1B). In contrast, later time points, in
126 particular 168 h, shifted to a less even viral community, with higher relative abundances of fewer
127 vOTUs. Average vOTU richness, as measured through the number of unique vOTUs per time
128 point, decreased significantly after 3 h (linear regression – *p value* = 0.02; R^2 = 0.28) (Figure
129 2B). While the number of vOTUs decreased by nearly 50% one-week post wetting, viral
130 biomass increased by at least four-fold (Figure 2C). We found viral biomass, as proxied by
131 measuring total extracted viral DNA through time, significantly increased after a week (linear
132 regression – *p value* = 2.1×10^{-3}; R^2 = 0.46).

133

134 To dissect temporal viral succession trends, we focused on the set of vOTUs that were present
135 in at least three time points within each replicate, i.e., “persistent vOTUs.” In previous studies
136 we observed phylum-specific succession in response to wet-up[20,23,49]. We hypothesized that
137 persistent vOTUs would reflect host dynamics and show similar temporal response patterns. We
138 established groups of vOTUs that behaved similarly across wet-up by hierarchical clustering of
139 relative abundance (Supplementary Figure 2). This clustering demonstrated several broad
140 patterns of abundance dynamics consistent across replicates: 1) vOTUs present early in wet-up
141 (0 h, 3 h, 24 h) that then disappear or drastically decrease in abundance i.e. early vOTUs; 2)
142 vOTUs that appear for the first time at 48h, i.e. late responding vOTUs; 3) vOTUs that are
143 present across all time points throughout the wet-up, i.e. ubiquitous vOTUs; 4) vOTUs that are
144 present in dry soil (time 0) and at the end of the wet-up time course (168 h), but are not
145 detected in all time points in between, i.e. 0 h and 168 h vOTUs. vOTUs that did not fit into
146 these categories were included in the “other” category (Supplementary Figure 3A). Each of
147 these defined response categories represented up to 15% of the total virome reads. Overall, we
148 observed that viral successional patterns responding to wet-up followed field plot-specific trends
149 (Figure 2, Supplementary Figure 1-3).

150

151 We hypothesized that vOTUs would reflect their host responses to rewetting and target
152 *Actinobacteria* and *Proteobacteria* as growing bacteria are expected to be targeted by viruses
153 based on the “kill the winner” hypothesis[51]. While host phylum-level analyses of viruses do not
154 reflect known viral host ranges (which are thought to be often on a strain level)[1,52], wet-up shows
155 consistent phylum-level microbial responses and host analyses were limited to coarser
156 taxonomic predictions (see Discussion). We examined the vOTU putative host composition
157 within each response group (Supplementary Figure 3B) and found vOTUs infecting
158 *Actinobacteria* dominated the groups responding immediately and after 24 hours.

159 *Alphaproteobacteria*-infecting vOTUs were the second most numerous vOTUs across nearly all
160 response groups. Overall, we found that vOTUs of prevalent hosts in our system (*Actinobacteria*
161 and *Proteobacteria*) appeared as the most prevalent vOTUs in each response category, but we
162 did not observe viral signatures of host-specific successional dynamics previously detected of
163 bacteria following wet-up[20,23].
164
165 We were curious whether late vOTUs (first detected as VLPs at 48 hours) represented earlier
166 viral infections. We predicted that these late viruses could be found inside microbial cells or
167 integrated into host chromosomes and tested this by analyzing whether these vOTUs were
168 detected in the cellular fraction, i.e. in metagenomes, prior to 48 hours. However, metagenome
169 reads from time points 0 h and 24 h did not map to late vOTUs in a manner that aligned with this
170 hypothesis (Supplementary Figure 4).
171
172 *Active virus-host dynamics illuminated with qSIP*
173
174 To assess the ecological role of viruses during this highly dynamic moment in the soil
175 microbiome we focused on the active subset of viruses and their microbial hosts. We defined
176 activity as incorporating ^{18}O from the $H_2{}^{18}O$ wet-up (Figure 1) and applied qSIP formulas to
177 quantitate genome isotopic enrichment (atom percent excess, APE) of DNA[40,41]. We
178 hypothesized that relating viral and host activity following rewetting may reveal to what extent
179 soil viruses follow canonical Lotka-Volterra oscillations, i.e., host activity peaks and precedes
180 peak viral activity (Figure 3A).
181
182 Given the prevalence of MAGs and vOTUs with a taxonomy or host-level taxonomy assignment
183 of *Actinobacteria* and *Proteobacteria*, and the previous high degrees of mortality and growth
184 following wet-up calculated for these lineage[23], we highlighted analyses comparing vOTUs and

185 MAGs of these lineages. Specifically, within Proteobacteria we focused on Alpha- and Gamma-
186 proteobacteria as growth could not be detected for other classes within this phylum in our
187 experiment. Rather than reflecting Lotka-Volterra predator-prey type dynamics, we observed
188 distinct lineage-specific predatory-prey dynamics (Figure 3). Active vOTUs predicted to infect
189 *Actinobacteria* showed higher activity than their MAG hosts in the first 48 hours, then their
190 activity decreased while MAG activity increased. This appeared to display a reversed Lotka-
191 Volterra dynamic[53]. Meanwhile, the activity of vOTUs predicted to infect the *Proteobacteria*
192 lineages followed the same temporal trend as host activity did, conceptually shown in the
193 bottom panel of Figure 3A[54].
194
195 The number of detected active MAGs and vOTUs follow similar temporal trends for all three
196 lineages we focused on (Figure 3C). For both *Actinobacteria* and *Proteobacteria*, there were
197 higher counts of active vOTUs than their hosts at nearly all time points. At 24 hours, for
198 instance, there were more than twice as many vOTUs as MAGs for all lineages, and for
199 *Actinobacteria* in particular, over fifteen times as many vOTUs were detected as isotopically
200 enriched compared to MAGs. Overall, for both MAGs and vOTUs, we found the greatest
201 number of newly detected active genomes at 48h. We similarly analyzed other phyla using
202 these metrics of MAG APE, vOTU APE, number of enriched genomes through time and found
203 no discernable patterns. Of note, from the 177 total enriched vOTUs detected in metagenomes,
204 58 were found in VLP viromes, indicating that at least 33% of viruses replicating and
205 assimilating isotope within host cells were also detected as putative virions within the
206 experimental timeframe.
207
208 *Viral lifestyle characterization*
209

210 To discern the mechanism for how viruses may exist, persist, and control host populations
211 following wet-up we investigated the lysogenic potential of vOTUs. To test our hypothesis that
212 wet-up induces temperate viruses we searched for vOTU genomes found in both viromes and
213 metagenomes that contained bacterial flanking regions in metagenomes to discover and
214 quantify lysogeny in our system (see Methods). This strategy yielded just two candidates of
215 vOTUs found both as VLPs in the virome and as putative prophage in metagenome contigs and
216 only one of these candidates was successfully binned into a MAG, a *Gammaproteobacteria* of
217 the genus *Pantoea*. The unbinned sequence was predicted to be an *Alphaproteobacteria*,
218 *Rhizobium leguminosarum*. We did not further characterize this binned putative prophage – it
219 was only detected in one plot at two non-consecutive time points (0 and 24h).
220
221 Unsuccessful in finding vOTUs appearing as both integrated in MAGs or bacterial sequences
222 and as VLPs, we examined our system for temperate phage by analyzing the genomic capacity
223 of vOTUs to integrate, via an integrase gene, into a host chromosome (Figure 4). Of the total
224 vOTUs detected 17% (4,463) contained an integrase gene and were denoted as putative
225 prophages. Non-integrase encoding vOTUs represented the majority of total viromes and
226 appeared responsive to wet-up, whereas integrase-encoding vOTUs decreased in proportion
227 following wet-up. Further, non-integrase encoding vOTUs were more numerous at all time
228 points (Figure 4B).
229
230 Concerned that vOTU contigs may be partial viral genomes left fragmented during assembly,
231 we also split the results of integrase-encoding and -lacking viral genomes by vOTUs that
232 circularize, implying genomic completeness, and vOTUs that are linear, and thus may or may
233 not be complete. We found that the linear set of vOTUs followed similar trends to circularized
234 vOTUs, therefore our observed dynamics suggest biological trends rather than artifacts of
235 incomplete assembly (Supplementary Figure 5).

236

237 We hypothesized that if lysogeny was a predominant mechanism of viruses responding to wet-
238 up then vOTUs appearing after wet-up (0 h) would be enriched in integrase genes, as vOTUs
239 appearing for the first time following wet-up may be prophages excised from genomes.
240 However, post-wet-up detected vOTUs were not significantly enriched in integrase genes
241 compared to vOTUs in dry soil (Chi-square test – *statistic* = 1.6; *p value* = 0.2).
242

243 To further support the inference that wet-up does not induce temperate viruses in this system,
244 we took a MAG-centric approach, and predicted prophages in the context of bacterial genomes
245 to discern how many (counts), and how prevalent (abundant) prophages are in this system
246 (Supplementary Figure 6). We analyzed detected prophage per phylum using aggregated
247 relative abundance of MAGs per time point and the count of total MAGs containing prophages.
248 Most phyla contained a predicted prophage, but prophage-containing MAGs for each phylum
249 were fewer and less abundant than MAGs without prophages. We next identified just three
250 prophages that seemed to be actively replicating based on coverage differences between
251 prophage sequences and their flanking host genomic regions[55]. One of these prophages
252 appeared active at all time points in at least two out of the three replicates, and was integrated
253 into a MAG of *Alphaproteobacteria* genus *Microvirga*. The other two prophages were active only
254 in a single replicate and in either one or two time points, and were integrated into genomes of
255 *Actinobacteria* family *Gaiellaceae* and *Alphaproteobacteria* family *Xanthobacteraceae*,
256 respectively.
257

258 To further investigate viral lifestyle and assess whether VLPs correspond to lysis we looked for
259 evidence for *Inoviridae*, known to cause chronic infections that do not lyse the host. We
260 performed an HMM search using the pI-like ATPase protein family HMM, which is conserved in
261 filamentous inoviruses[56], and found no evidence of *Inoviridae* in our viromes or metagenomes.

262

263 *Quantifying viral contribution to microbial mortality*

264 We approximated the viral contribution to mortality following wet-up using VLP sequence data
265 from this work and bacterial mortality estimates from corresponding SIP-density fractionated
266 amplicon sequencing[49]. We modeled a range of viral burst sizes based on existing literature
267 from one virus released per cell lysed[2,57] to 200 viruses released per cell lysed[58]. Taken
268 cumulatively, at 168 hours viral contribution to microbial death ranged from 0.25% (burst size of
269 200) to 46.6% (burst size of 1) (Figure 5B). At 24 hours we observed the highest per day viral
270 contribution to microbial mortality 0.02% (burst size of 200) to 17.4% (burst size of 1).

271

272 **DISCUSSION**

273

274 Soil is a highly complex microbial habitat and home to tens of millions of microbial
275 populations[59,60], where biotic and abiotic factors shape microbial community structure[61–63].
276 Moments of acute pressure on a community, such as rapid environmental changes or fluxes in
277 resource availability, drive successional trajectories that result in altered community structures;
278 the first rainfall following the dry season, wet-up, is such a moment[19,23,38,64,65]. However, the
279 ecology, lifestyle, and impact of viruses in the soil microbiome during dynamic moments
280 remains unknown. To address this gap in knowledge, we applied viromics and SIP targeted
281 metagenomics to: 1) assess viral biomass and richness following rewetting and posited that dry
282 soil may serve as a seedbank of virions for the growing season; 2) analyze dynamics of active
283 viruses and found lineage-specific host trends where viruses may follow host populations or
284 control them; 3) investigate viral life cycle and observed minimal evidence for lysogeny
285 suggesting a lytic lifestyle is predominant following wet-up; 4) estimate viral contribution to
286 microbial mortality discovering viral contribution steadily increases following rewetting.

287

288 In response to rewetting, we observed a large decline in viral richness, and by extension
289 diversity, in the first 24 hours, which was inversely related to an increase in viral biomass
290 (Figure 5A). This pattern was consistent across all soil replicates making it detectable despite
291 the high degree of inter-sample heterogeneity (Figure 2A, Supplementary Figure 1). We
292 observed viral populations may degrade or thrive following rewetting, but after one week post
293 perturbation viral composition across plots did not become more similar. Rather, the virions
294 present at the end of the dry season determined the trajectory of the plot-specific viral
295 composition. At this timescale and sampling, wet-up is not a perturbation at which we observed
296 a convergence of viral populations across space despite relative host uniformity at the same
297 sampling (Figure 2). These results imply that dry soil may be a reservoir, or seedbank, of
298 diverse viruses, a subset of which becomes dynamic following rewetting (Figure 2,
299 Supplementary Figure 1B).

300

301 Intriguingly, analysis of the total viral pool responding to wet-up revealed patterns of succession,
302 but viral succession did not appear to be correspondent with known host responses previously
303 reported and observed in our corresponding study (Supplementary Figure 2-3)[20,23,49]. However,
304 focusing on the active subset of microbial and viral populations (Figure 3), we found taxon-
305 specific trends in viral-host dynamics wherein viruses may follow their microbial hosts or,
306 perhaps, control host populations. Studies from marine systems have shown that viruses may
307 follow their hosts' dynamics[54] and that high local diversity of viruses may be drawn from a
308 seedbank of nearby viruses[8]. As suggested in Chow et al.[54], our isotope targeted results
309 indicate that viruses putatively infecting *Alphaproteobacteria* follow their host dynamics, as
310 opposed to viruses directly controlling host activity or abundances. On the other hand,
311 *Actinobacteria*-infecting viruses appear to show a reversed Lotka-Volterra relationship which is
312 suggestive of coevolution driven dynamics[53]. Broadly, the total responding pool of putative

313 virions does not necessarily match the total microbial response to rewetting, therefore it is
314 important to focus on the active subset of vOTUs and MAGs to appreciate host-virus dynamics
315 in this soil system. Our study provides a first glimpse into fine spatiotemporal viral dynamics in
316 soil and enabled us to categorize distinct viral responses to rewetting.
317
318 Critical to understanding how viruses respond to wet-up and impact the soil microbiome is an
319 analysis of the mechanism of viral life and survival in soil. An emerging idea in soil viral ecology
320 suggests that lysogens, or temperate viruses, are prevalent in soil microbes, and further, that
321 lysogeny is a favorable lifestyle for viruses both to remain linked to a host and to weather
322 conditions difficult for growth, i.e., dry soil[1,2,5,6,29,35,60,66,67]. We tested this hypothesis looking
323 specifically at wet-up as an environmental perturbation that could induce prophage and found
324 no evidence to support this hypothesis.
325
326 Rather, our data suggests that vOTUs which cannot recombine into a host chromosome through
327 an integrase dominate this system. We found no clear evidence showing wet-up significantly
328 induces prophages. The viruses that do increase in abundance following the first 24 hours are
329 predominantly non-integrase encoding. We hypothesized that late-responding vOTUs may also
330 provide a window into viral life strategies (Supplementary Figure 3A) – that examining virome
331 late-responders in metagenomes would reveal these viruses were cell-associated prior to
332 appearance as VLPs. As late-responding viruses did not appear in metagenomes at earlier time
333 points at higher abundances than in later time points (Supplementary Figure 4); temperate
334 viruses did not predominate as responding viruses to wet-up; and prevalent MAGs did not
335 maintain detectable or active prophages (Supplementary Figure 6) we conclude that neither
336 lysogeny as a lifestyle nor temperate phages in general dominate during wet-up in this soil
337 system.
338

339 Whether all detected VLPs in our system originate from cell lysis events remains unclear. While
340 we did not find evidence of *Inoviridae* – viruses that can replicate and release virions without
341 lysing their hosts through a chronic infection[56], other non-lytic lifestyles may be possible.
342 Further, while neither the capacity to integrate into a host chromosome nor persistence as a
343 prophage is prevalent in our wet-up study, we were not able to rule out other mechanisms of
344 viral maintenance in a host cell when a virus is not lytically programmed, e.g.,
345 pseudolysogeny[68]. Perhaps evidencing the prevalence of pseudolysogeny or some other cell-
346 associated state of soil viruses, the majority (67%) of viral populations detected as active were
347 only found in metagenomes (direct DNA extraction from soil) rather than viromes. For a virus to
348 be detected as enriched it must be infecting host cells to replicate, thus assimilating the ^{18}O
349 isotope. Most of these active viruses may not be detected in the viromes (i.e., as putative
350 virions) because of their host-associated state. Importantly, the low fraction of persistent vOTUs
351 (Supplementary Figure 2-3) compared to total vOTUs suggests virome-detected viruses may
352 indeed derive from recent host infections.
353
354 Microbial death is critical to the flow of nutrients through biomes[60]. A significant feature of soil
355 wet-up is high rates of microbial mortality[19,21,23]. Our previous work demonstrated rapid bacterial
356 mortality following wet-up, with 25% of bacteria degrading in the first 3 hours and continued
357 mortality observed through 72 hours[21]. We hypothesized that the initial burst of mortality in the
358 first 3 hours was driven by osmotic lysis due to the rapid change in osmotic pressure, while
359 mortality after 3 hours was driven by viruses or other biological factors[19]. Others have also
360 speculated that viruses play a role in observed mortality following rewetting[69]. We found that
361 viruses play a minor role in mortality in the first 3 hours, when osmotic lysis is likely the
362 dominant mechanism of lysis, and the contribution to mortality by viruses increases through
363 time, more than doubling after the first 24 hours (Figure 5B). We estimate that viruses can drive
364 a sizeable portion of microbial mortality in soil – by 168 hours viral-mediated mortality may

365 contribute 0.23 % to 46.6 % of total microbial death dependent on burst size estimated. While
366 our evidence suggests viruses play an important role in microbial mortality following wet-up, we
367 infer that this influence is minimized as wet-up led to a rapid decline of viral particles in the first
368 24 hours (Figure 2B-C). If viral biomass continues to increase following 168 hours post wet-up,
369 we posit that the viral contribution to microbial mortality may be higher. Our estimate of viral
370 driven mortality in the soil microbiome aligns with estimates from marine systems ranging from
371 undetectable to majority of mortality is viral or the more commonly cited estimate via microscopy
372 of 20 - 40 % of bacteria daily lysed by viruses[10,70,71]. There may also be other circumstances in
373 the soil microbiome where viruses play a larger role in mediating microbial death, perhaps in the
374 rhizosphere, where turnover of cells is faster[72,73]. Further studies are required to improve our
375 calculations by constraining the average genome length of soil viruses, range of viral burst sizes
376 in soil, and how long VLPs persist in soil to understand whether virions represent recent
377 infections or whether these calculations require techniques that capture an active fraction of
378 viruses. Moreover, viral predation has impacts beyond contribution to mortality broadly. Even
379 low viral turnover rates of key lineages may profoundly impact strain selection and functional
380 potential of soil microbiomes.
381
382 Our data show spatial heterogeneity is an important feature in understanding the response of
383 viruses to rewetting. While a rapid decline in viral diversity, increase in viral biomass, and
384 successional patterns emerged as trends across the studied soil plots, the majority (59%) of
385 viruses appeared in fewer than three of our total 18 viromes and most do not appear in all
386 biological replicates (Supplementary Figure 1). The patchiness of viruses across plots precluded
387 tracking subsets of viruses through space and time to find statistically meaningful trends. The
388 heterogeneity of soil viruses suggests that infection may not be as uniform across space as
389 potential hosts are. Perhaps, this is the effect of rewetting: virions persisting in soil, may be
390 decoupled from their hosts, and the addition of water may exacerbate the hurdle of host-viral

391 physical interactions as previous research has predicted increased water potential is associated
392 with lower rates of direct cell-cell contact in soil[74]. On the other hand, wet-up may serve to
393 increase connectivity between soil microsites and relieve dispersal limitations of viruses,
394 promoting host encounters. As research has shown, water may constrain microbial or viral
395 dispersal[75,76]. Our observed increase of viral biomass following wet-up suggests water would
396 support physical interactions between viruses and their hosts.
397
398 The viral heterogeneity observed throughout our field site[77] also raises questions about our own
399 assumptions in the design of this experiment: that the field plot layout, informed by bacterial
400 biogeography would enable similar trends for viruses. Rather, our fine time-resolved study and
401 concurrent work studying heterogeneity on a field scale at longer time intervals[77] have
402 compelled us to question what scale of sampling for viruses represents biological replicates.
403 Our results suggest that future studies should consider the distinct scales of microbial and viral
404 populations in soil to have a holistic understanding of microbial communities[66].
405
406 Given the higher spatial homogeneity in microbial distribution and response to rewetting
407 compared to viral distribution (majority of MAGs appear in all samples, Supplementary Figure
408 1), it is tempting to hypothesize that this indicates microbes in soil are widely susceptible to
409 infection by many distinct viral populations. However, the lack of specific host-virus linkages in
410 our system prevented investigation of viral host breadth.
411
412 Linking individual viruses to their specific host genomes remains a challenge in ecovirology.
413 Using mixed methods and multiple databases we were able to determine at least a domain or
414 phylum-level taxonomy for 93% of vOTUs. We found few CRISPR spacer matches[78] and were
415 only able to directly link vOTUs to specific MAGs with high confidence in a few instances. Thus,
416 current limitations in informatics precluded us from directly implicating viruses as preying on

417 specific MAGs and track predator-prey dynamics on a strain level. Our phylum-level viral-host
418 predictions revealed that the most numerous and prevalent viruses in our system infected
419 *Actinobacteria* and *Proteobacteria*, which reflected the microbial community – the most common
420 viruses infected the most common hosts – implying that viruses may serve an important
421 regulatory role in soil microbial communities. Further, we were able to observe lineage-specific
422 viral-host dynamics on the phylum level which demonstrated that there is not a single mode of
423 viral impact on hosts. Instead, in a complex system, we found multiple models of virus-host
424 dynamics. Taken together, these observations suggest viruses exhibit lineage-specific impacts
425 on host populations and thus viruses serve an important role in structuring the soil microbiome.
426
427 In this work, we probed the wet-up of a seasonally dry soil to understand the role of viruses in
428 microbiome assembly. We found that dry soil is a low biomass yet highly rich seedbank of
429 unique virions, and that resuscitation of the microbiome yields a bloom in biomass of a subset of
430 viruses. Succession of the total pool of viruses is driven by spatial heterogeneity. We observed
431 that, on a phylum level, active viral populations show distinct models of impact on hosts.
432 Further, contrary to the emerging paradigm, our data show that lysogeny is not prevalent in our
433 system, underscoring that the reservoir of soil viruses may rely on other forms of host
434 interactions or on virions rather than as inserts in microbial genomes. Our combined use of
435 viromics, metagenomics, and isotope tracing facilitated estimation of the viral contribution to
436 microbial mortality following rewetting. While our conservative calculations indicate viruses may
437 not be the primary mechanism of observed mortality, viruses appear to play an important and
438 dynamic role in the microbial response following wet-up.
439
440 **METHODS**
441
442 *Field sample collection*

443 Topsoil samples (0-15 cm, roughly 0.5 m^3) from replicate field plots were collected from the
444 Hopland Research and Extension Center (HREC) in Northern California, which is unceded land
445 of the Shóqowa and Hopland People, on August 28th, 2018 after experiencing mean annual
446 precipitation during the rainy season, see our paired study Sieradzki et al. 2022[49] for full details.
447 During the growing season the same field plots were covered by mixed grassland flora with
448 *Avena sp*. (wild oat) as the most abundant plant. Soil was collected before the first rainfall event
449 of the season and average gravimetric soil moisture was 3%. The dry soil was transferred to
450 Lawrence Livermore National Laboratory (LLNL) where it was homogenized and sieved (2mm)
451 to remove large rocks and roots.
452
453 *Wet-up experiment*
454 Stable isotope probing (SIP) is a method for tracking the incorporation of an isotope into the
455 DNA of replicating organisms via ultracentrifugation (Beckman-Coultier (Indianapolis, IN, USA)
456 VTi 65.2 rotor at 44,100 rpm for 109 h at 20ºC) of the DNA in a density gradient. DNA
457 equilibrates in the gradient according to its GC content and isotopic enrichment. The gradient is
458 then divided into density fractions each of which is analyzed for density (handheld AR200 digital
459 refractometer), amount of DNA (PicoGreen assay (Life Technologies)) and community
460 composition (in this case shotgun metagenomics). 5 g sieved soil from each of 3 field replicates
461 was weighed into separate 15 mL Nalgene flat bottom vials. Soil was wetted to 22% average
462 gravimetric soil moisture with either $H_2{}^{18}O$ (98 atom% ^{18}O) or $H_2{}^{16}O$ (natural abundance SIP)
463 controls) (Figure 1), after which the vials were sealed inside 500 mL mason jars and incubated
464 at room temperature in the dark. Three incubation treatments were established, each in
465 triplicate: 1) $H_2{}^{16}O$ amended (used for DNA extraction, unfractionated DNA shotgun sequencing
466 and as a fractionated DNA control for qSIP); 2) watered with $H_2{}^{18}O$ for DNA extraction, density
467 centrifugation, and shotgun sequencing (isotopically-labeled fractionated DNA for qSIP); 3)
468 watered with $H_2{}^{16}O$ for viral-like particle (VLP) suspension, concentration, DNAse treatment

469 followed by DNA extraction and shotgun sequencing to generate viromes (unfractionated DNA
470 for viromics). Parallel jars were destructively harvested at 0, 3, 24, 48, 72, and 168 hours
471 following the water addition; at each harvest, soil vials were frozen in liquid nitrogen and then
472 stored at -80 °C.
473
474 *Viral metagenomes ("viromes")*
475 Soil viromes were generated as described in Nicolas et al. 2021[50] to assess viruses detected as
476 VLPs i.e. extracellularized. Briefly, two 5-gram soil microcosms from each of three field
477 replicates watered with $H_2{}^{16}O$ were combined for 10 g soil virome extractions. Soil was buffered
478 with a potassium citrate solution and the effluent was passed through a 0.2-µm filter,
479 concentrated, and treated with DNase to remove extracellular DNA. Prior to DNA extraction
480 using a phenol:chloroform strategy, we used an iron flocculation step to concentrate 0.2-µm
481 filtered and concentrated samples as described in Nicolas et al. 2021[50]. DNA was sequenced on
482 an Illumina Novaseq (2x150 cycles) (UC Davis). Sequencing was performed to attain an
483 average 40 Gb per sample. Illumina adapters and phiX were removed from resulting sequences
484 using BBTools (https://jgi.doe.gov/data-and-tools/bbtools/) and then quality trimmed using
485 Sickle[79]. Sequences were assembled with MEGAHIT version 1.2.9[80]; we co-assembled all
486 biological replicates per time point using default parameters. Open reading frames (ORF) were
487 predicted for each contig using Prodigal[81] and were annotated using sequence similarity
488 searches with USEARCH[82] to KEGG[83], uniref[84], and uniport[85].
489
490 *Metagenome assembled genomes (MAGs) from viromes*
491 To generate microbial bins from the size-fractionated metagenomes, i.e. viromes, we used
492 multiple binning methods. Contigs were binned using Maxbin[86], MetaBAT[87], Concoct[88], and
493 manually based on coverage, GC content, and taxonomy using in house tools on ggkbase
494 (https://ggkbase.berkeley.edu). DASTool[89] was used to predict best bins and bins were further

495 manually curated on ggKbase to remove highly divergent sequences based on coverage, GC,
496 and taxonomy. MAGs from viromes were clustered and dereplicated alongside MAGs from
497 metagenomes (discussed below) using dRep[90] requiring at least 75% completeness and no
498 more than 10% contamination, yielding 39 genomes from candidate phyla radiation bacteria and
499 archaea.
500
501 *Viral prediction and generation of viral operational taxonomic unit (vOTU) set*
502 To establish a set of viral genomes from our metagenomic efforts we used multiple methods of
503 prediction and dereplicated vOTUs across samples. Viruses were predicted from metagenome
504 and virome contigs. Viruses were predicted using: virsorter1[91] (all categories), virsorter2[92]
505 (dsDNA and ssDNA only), VIBRANT[93], deepvirfinder[94] (score ≥ 0.9; pvalue ≤ 0.05), and
506 seeker[95]. From the set of virome and metagenome contigs explored 3,979,792 were predicted
507 to be viral. Of these, 777,725 contigs were designated viral by more than one tool, and 32,660
508 of this subset were either circularized contigs by VRCA[96] (i.e. implied to be a complete
509 genome), or ≥ 10,000 base pairs long. This set of size-filtered, circularized, repeatedly predicted
510 viruses was dereplicated using mmseqs (95% ANI, 85% breadth required of sequences) to
511 26,368 viral operational taxonomic units (vOTUs). All vOTUs were annotated using DRAM-v[97],
512 and specifically searched for integrase genes.
513
514 *DNA density fractionation*
515 DNA was extracted from three biological replicates at each time point using a modified phenol-
516 chloroform protocol adapted from Barnard et al. (2015)[98] as described in[49]. For density gradient
517 SIP processing, 5 µg of DNA in 150 µL 1xTE was mixed with 1.00 mL gradient buffer, and 4.60
518 mL CsCl stock (1.885 g mL^{-1}) with a final average density of 1.730 g mL^{-1} as described in
519 Sieradzki et al (68).The fractions for each sample were binned into 5 groups based on density
520 (1.6400-1.7039 g/ml, 1.7040-1.7169 g/ml, 1.7170-1.7299 g/ml, 1.7300-1.7449 g/ml, 1.450-

521 1.7800 g/ml), and fractions within a binned group were combined and sequenced.
522 Unfractionated DNA (100 ng) from each soil sample was also saved for shotgun sequencing.
523 All sequencing was performed on an Illumina Novaseq 2x150 cycles. Pre-aliquoted
524 unfractionated DNA from each sample was sequenced to an average of 20 Gb per sample, and
525 DNA from each binned group of density fractions was sequenced to an average of 10 Gb per
526 binned group, yielding a total of 227 metagenomes. Illumina adapters and phiX were removed
527 using BBTools and reads were quality trimmed using Sickle using default parameters.
528
529 *Metagenome assembly, annotation, and binning*
530 To establish MAGs from metagenomes we approached assembly in two ways: 1) co-assembly
531 of unfractionated triplicates for each time point 2) co-assembly of the 5 density fractions from
532 each time point and each replicate. We used MEGAHIT version 1.2.9 for assemblies[80] with
533 preset large-meta and disconnect ratio 0.33[49]. Metawrap version 1.3.2[99] was used to map reads
534 from unfractionated metagenomes to contigs from each assembly, bin each assembly with
535 MetaBAT2[87] and Maxbin2[86] and refine bins. Genomic bins from all samples as well as bins from
536 soil metagenomes collected at the same site in the preceding winter[40] were then dereplicated at
537 95% average nucleotide identity (ANI) using dRep version 3.0.1[90] to create a final collection of
538 high quality 503 metagenome assembled genomes (MAGs) that were on average 87%
539 complete and 5% redundant. Taxonomy was assigned to bins using GTDB-tk version 1.5.1[100].
540
541 To calculate abundance measurements for MAGs, reads from unfractionated samples were
542 mapped back to the MAG collection using bbmap with minid=0.98 (https://jgi.doe.gov/data-and-
543 tools/bbtools/). Mapping statistics were then used to calculate coverage at reads per kilobase
544 million (RPKM), mapped read counts and breadth of coverage using CoverM
545 (https://github.com/wwood/CoverM), and were normalized to sequencing depth.
546

547 *Calculating relative abundances of the vOTU collection*

548 To quantify abundance of vOTUs in viromes and metagenomes and to assess activity via qSIP
549 we mapped reads from these sequencing efforts to our vOTUs. All reads from viromes,
550 metagenomes, and SIP-fractionated metagenomes were mapped to the set of vOTUs using
551 bbwrap.sh at 98% minimum identity. Samtools[101] sort and index functions were applied to
552 resulting bam files. We used CoverM to calculate breadth and read count per vOTU per sample.
553 Read counts were divided by total reads per sample to calculate relative abundance. For virome
554 relative abundance we considered vOTUs present in a sample if they had at least 80% breadth
555 covered (fraction of genome covered by reads). For use with the qSIP pipeline, we found that
556 few vOTUs had reads that mapped stringently (98% identity) and in all three replicates of
557 multiple density fractions in both ^{18}O and ^{16}O conditions and therefore chose a lower breadth
558 cutoff, 50%, for detection of vOTUs in SIP fractions (described below).

559

560 *Ordination plots*

561 To understand compositional differences through time responding to rewetting we constructed
562 ordination plots. For MAGs we constructed a matrix of metagenome relative abundance per
563 sample per genome. Similarly for vOTUs, we generated a matrix of relative abundance per
564 sample per genome, using vOTU relative abundance as calculated from our virome samples.
565 We used the python scikit package[102] to calculate Bray-Curtis dissimilarity and to perform
566 principal coordinates analysis (PCoA) to visualize the dissimilarity between samples.

567

568 *Virus-host linkage and assigning viruses a host taxonomy*

569 To link vOTUs to potential host microbial MAGs, we used multiple approaches, starting with
570 CRISPR spacer searches. We predicted CRISPR arrays using minced
571 (https://github.com/ctSkennerton/minced)[103] in the original set of MAGs (not dereplicated) from
572 this study, in MAGs from another qSIP study conducted in a soil from our field site[40], and in our

573 viromes. 84 MAGs and 32 vOTUs contained CRISPR arrays with at least 1 spacer. We aligned
574 the MAG spacers against the vOTUs using BLASTn[104], and vice versa, and screened for hits
575 with no more than one mismatch and no gaps between the full spacer and the vOTU. By these
576 criteria, only one vOTU spacer matched a MAG in our dataset. This vOTU appeared in two of
577 three plots and in two time points for each plot. In contrast, 25 MAG spacers from 6 MAGs
578 matched 19 vOTUs. From these linkages we assigned host taxonomies to vOTUs using the
579 associated MAGs GTDB taxonomy[100].
580
581 To assign host taxonomy to additional vOTUs we combined these CRISPR spacer searches in
582 MAGs, with a broader set of CRISPR spacer matches, and contig taxonomy predictions. In
583 addition to MAG and vOTU spacers, we also predicted spacers in unbinned metagenome
584 contigs using minced and established contig taxonomy for these unbinned contigs using
585 Kaiju[105]. We used the same BLAST parameters to match these unbinned CRISPR array
586 spacers to our dereplicated vOTU set. Next, we queried the comprehensive spacer database
587 generated in Shmakov et al. 2017[106] against our vOTU sequences using the same BLAST
588 parameters. Each spacer from this database[106] included an NCBI taxonomy that was assigned
589 to matching vOTU protospacers as the host taxonomy.
590
591 We also used vOTU sequences to inform host taxonomy. Previously, Al-Shayeb et al. 2020 and
592 others assigned host phyla to phages based on whether ORF annotations in phages were
593 predominantly of one phylum[107]. Here, we used Kaiju on vOTUs to assess taxonomy. Most
594 vOTUs were assigned to microbial taxonomies that presumably reflect shared host-virus
595 genome/gene content. We used this microbial taxonomic assignment to set a putative host. For
596 vOTUs predicted to have viral taxonomies we captured host lineages using the Virus-Host
597 Database[108].
598

599 Lastly, we created a database of all vOTUs, their host predictions, and the source of each host
600 prediction – CRISPR spacer-based taxonomy from GTDB for MAGs, unbinned spacers with
601 Kaiju taxonomic predictions, NCBI taxonomies from spacers matched from the spacer database
602 used, or Kaiju taxonomy predictions per vOTU. We used this database to determine the
603 consensus taxonomy between these sources closest to a species level by searching for the
604 greatest common denominator level of taxonomy. This allowed us to find putative hosts for
605 93.1% of total vOTUs at the domain level, and 92.8% at the phylum level. We also attempted
606 link specific MAGs and vOTUs using a network-based analysis modelling canonical predator-
607 prey dynamics, but were unsuccessful in ground truthing these linkages and thus did not include
608 these host matches.
609
610 *Examination of evidence for viral induction*
611 The following methods largely describe negative results, however we chose to disclose these
612 methods to provide information for method developments for the benefit of the scientific
613 community. To quantify viruses in our system that were present both as prophages in MAGs
614 and as VLPs in the virome we mapped virome reads to metagenomes and looked for alignment
615 between metagenome sequences and vOTUs. Specifically, we mapped all virome reads to
616 metagenome assembled sequences at 90% average nucleotide identity. We used coverM
617 (https://github.com/wwood/CoverM) to generate breadth and coverage calculations for mapped
618 reads and identify metagenome contigs that had virome reads mapping with at least 1000 bp
619 covered by reads, but not mapping with 100% breadth. We believed this implied that reads
620 mapped to a potential lysogenic viral genome embedded in the host genome. Using BLASTn
621 [104], we aligned the set of metagenome contigs that met these criteria against our vOTUs with a
622 minimum E-value of 10^{-100}. We subsetted the resulting matches to vOTUs that matched a
623 metagenome contig with greater than 90% nucleotide identity, aligned with a metagenome
624 sequence that had more than 10 Kbp of flanking region around the alignment, and an aligned

625 section of at least 10 Kbp. This resulted in 11 vOTUs representing candidate lysogenic viruses.
626 Using ggKbase (https://ggkbase.berkeley.edu/), we manually analyzed each of these vOTUs
627 and their corresponding metagenome contigs for aligned and unaligned regions consistent with
628 phage (enriched for hypothetical genes, viral structural genes, integrase genes). This resulted in
629 two sequences that appeared to be lysogenic: found both as vOTUs in viromes and in
630 metagenomes in the context of bacterial sequences.
631
632 *Assessment of prophages in MAGs*
633 Prophages were identified from our set of MAGs by virSorter version 1 categories 4 and 5[91], or
634 by VIBRANT[93]. Active prophages, i.e. prophages assessed as replicating more than their
635 flanking host genome, were identified by running PropagAtE[55] with metagenome read mapping
636 files to MAGs previously generated. PropagAtE relies on differential coverage between
637 prophage and flanking host regions.
638
639 *Viral response categories*
640 To establish viral response patterns through time, we constrained the set of vOTUs to 6,840
641 vOTUs present in a specific field plot for three or more time points; we refer to these as
642 "persistent vOTUs." We generated hierarchically clustered heatmaps (cluster maps) per field
643 plot in seaborn[109] using relative abundances per time point for each vOTU. With cluster map
644 observations and k-means clustering, we established 5 response categories based on vOTUs
645 presence or absence in given time points: 1) 'early vOTUs' present at 0 h, 3 h, and 24 h post
646 wet-up; 2) 'late responding vOTUs' present at 48 h, 72 h, and 168 h post wet-up; 3) 'ubiquitous
647 vOTUs' present in all time points; 4) 'vOTUs present at 0 h and 168 h' and one other time point;
648 5) 'other' vOTUs that did not fall into these categories. We summed vOTU relative abundances
649 across these categories for each time point per plot. We used the seaborn relplot function[109] to
650 visualize response categories through time per plot. To measure the host signal by response

651 category, we summed the unique vOTUs of a given bacterial putative host phylum or domain
652 per category. We visualized host abundances per response category by overlaying seaborn
653 swarmplots on boxplots where each point corresponds to a field plot.
654
655 *Construction of integrase-containing vOTUs relative abundance and richness barplot*
656 We used the seaborn relplot function[109] to construct graphs of vOTUs that did (4,463 unique
657 vOTUs) or did not contain integrase genes. We plotted the set of vOTUs split into these two
658 categories and by circular versus linear, by their aggregated relative abundance through time
659 and by vOTU richness per category through time.
660
661 *Quantitative stable isotope probing*
662 Atom percent excess (APE) isotopic enrichment values were calculated using quantitative
663 stable isotope probing (qSIP)[40,46,49] by normalizing MAG and vOTU relative abundance to the
664 quantity of DNA per density fraction[40]. Both bacterial and viral genomes were required to be
665 detected in all three replicates of each labeled ^{18}O treatment and in three replicates of unlabeled
666 (^{16}O) treatments for the bootstrapped median atom percent excess (APE) to be calculated per
667 genome. From the qSIP output we removed genomes with an APE median confidence interval
668 lower than 0 (i.e., not statistically significant). We plotted the average median APE MAG and
669 vOTU values through time for our most prevalent vOTU and host phyla – Actinobacteria,
670 Alphaproteobacteria, and Gammaproteobacteria – using seaborn line relplots. We enumerated
671 the number of detected enriched vOTU and MAG genomes and plotted these counts per
672 phylum through time.
673
674 *Viral contribution to microbial mortality*
675 We modeled the viral contribution to microbial mortality using a range of potential burst sizes
676 (virions per infected cell) to relate the number of approximated infectious viral particles through

677 time to observed microbial cell death counts. Counts of microbial cell mortality were derived
678 from our qSIP analysis of corresponding amplicon sequence data[49]. We used the median rate of
679 16S rRNA copies lost per gram soil per day and converted this rate to per gram soil by
680 multiplying by the number of days. To convert 16S rRNA copies to cells lost, we used a
681 conservative assumption of six rRNA copies per microbial cell[21,110]. The approximate loss of
682 microbial cells per gram of soil was used to represent the total observed microbial mortality. To
683 calculate the contribution of viruses to observed mortality, we estimated the number of total
684 virions per time point, using the mean aggregated relative abundance across plots (total reads
685 mapped to our vOTU dataset). We used the fraction of viral reads to estimate viral DNA of total
686 extracted DNA per time point per plot. With our estimate of viral DNA and a calculated mean
687 genome length in our vOTU dataset of 2.1254 x 10^4 bp, we used equation 1 (previously used to
688 estimate plasmid copy numbers from DNA) to calculate virions per time point:
689 (1)

690 $$\text{Virions} = \frac{\text{X ng} \times 6.0221 \times 10^{23}\,\frac{\text{molecules}}{\text{mole}}}{\text{N} \times 660\,\frac{\text{g}}{\text{mole}} \times 1 \times 10^{9}\,\frac{\text{ng}}{\text{g}}}$$

691 $X = Calculated\ viral\ DNA$

692 $N = Average\ calculated\ genome\ length\ (bp)$

693

694

695 As an average viral burst size in soils is unknown, we converted number of virions to cells lysed
696 by using a range of viral burst sizes from one virus released per cell[2,57] to 1000[58]. Virions scaled
697 to cells dead by the burst size range served as a numerator for viral contribution to microbial
698 mortality calculated with equation 2. We next captured cumulative viral contribution to microbial
699 mortality through time by taking the cumulative sum of all previous time points for each time
700 point.

701 (2)

702 $$Viral\ contribution\ to\ microbial\ mortality = \frac{Virions\ \times\ burst\ size}{\frac{degraded\ rRNA\ copies}{6}\ \times\ Days}$$

703

704 Our calculations made the following assumptions: 1) All virions detected lyse their host. 2)
705 Virions calculated for each time point represent new infections rather than virions persisting
706 through time i.e., virions were released from newly lysed cells. 3) Our VLP-virome extraction
707 protocol efficiently extracted 100% of soil viruses, i.e., viruses detected represent all possible
708 soil viruses. 4) The mean vOTU genome length represented an accurate approximation of soil
709 viral lengths irrespective of short read metagenomics and potential assembly fragmentation. Our
710 data supported the second assumption given that only a minority of vOTUs appeared in multiple
711 time points (Supplementary Figure 1). Further, we performed a sensitivity analysis of the impact
712 of genome length on our calculation and found a statistically significant relationship between
713 genome length and percent viral contribution to mortality (linear regression on log transformed
714 data, slope: -1.00, intercept: 7.80, r-value: -0.73, p-value: 6.63×10^{-07}) – changing viral genome
715 length by an order of magnitude led to an order of magnitude decrease in the percent
716 contribution to mortality.

717

718 **ACKNOWLEDGEMENTS**

719

720 This research was supported by the U.S. Department of Energy (DOE), Office of Biological and
721 Environmental Research (BER), Genomic Science Program Lawrence Livermore National
722 Laboratory (LLNL) 'Microbes Persist' Soil Microbiome Scientific Focus Area SCW1632, and a
723 subaward to UC Berkeley. Field plots and precipitation management were initially generated via
724 DOE BER awards DE-SC0020163 and DE-SC0016247 (to MKF) and awards SCW1589, and
725 SCW1421 (to JPR). Work at Lawrence Livermore National Laboratory was conducted under the

auspices of the U.S. DOE under contract DE-AC52-07NA27344. We acknowledge funding support to J.F.B. from the Chan Zuckerberg Biohub and the Innovative Genomics Institute at UC Berkeley.

We would like to thank Rachel Hestrin and Alexander Jaffe for helpful conversations regarding data analysis and visualization, and interpretations of isotopic data. We thank Katerina Estera-Molina for her expertise and management of the Firestone Lab field work site at the Hopland Research and Extension Center (HREC). Members of the Taga and Firestone labs provided helpful commentary and criticisms of this work. In particular, Mengting Maggie Yuan engaged in important conversations on statistical analyses. Rohan Sachdeva and Shufei Lei of the Banfield lab equipped this project with the necessary computational power and data management via the biotite server and ggKbase, respectively. Support staff at LLNL enabled the large-scale wet-up microcosm experiment and sample extractions, particularly Xiao Bin Max Li and Marissa Lafler.

We acknowledge that HREC sits on traditional, unceded land of the Pomo Indians. Research conducted at the University of California, Berkeley took place on the territory of xučyun (Huichin), the ancestral and unceded land of the Chochenyo-speaking Ohlone people, the successors of the sovereign Verona Band of Alameda County. This land was and continues to be of great importance to the Muwekma Ohlone Tribe and other familial descendants of the Verona Band.

J.F.B. is a founder of Metagenomi. The other authors declare no competing interests.

751 **DATA AVAILABILITY**

752 Raw data used in this publication is available on the NCBI short read archive under project
753 submission number SUB11697222. Viral genome sequences i.e., vOTUs are available on
754 ggkbase.berkeley.edu/project_groups/Hopland_4th_wedge. No custom tools were used to
755 analyze the data.

756

757 **REFERENCES**

758 1 Williamson KE, Fuhrmann JJ, Wommack KE, Radosevich M. Viruses in Soil Ecosystems:
759 An Unknown Quantity Within an Unexplored Territory. *Annual Review of Virology* 2017; 4:
760 201–219.

761 2 Kuzyakov Y, Mason-Jones K. Viruses in soil: Nano-scale undead drivers of microbial life,
762 biogeochemical turnover and ecosystem functions. *Soil Biology and Biochemistry* 2018;
763 127: 305–317.

764 3 Emerson JB, Roux S, Brum JR, Bolduc B, Woodcroft BJ, Jang H Bin *et al.* Host-linked
765 soil viral ecology along a permafrost thaw gradient. Nature Microbiology. 2018; 3: 870–
766 880.

767 4 Paez-Espino D, Eloe-Fadrosh EA, Pavlopoulos GA, Thomas AD, Huntemann M,
768 Mikhailova N *et al.* Uncovering Earth's virome. *Nature* 2016. doi:10.1038/nature19094.

769 5 Pratama AA, van Elsas JD. The 'Neglected' Soil Virome – Potential Role and Impact.
770 *Trends in Microbiology* 2018; 26: 649–662.

771 6 Emerson JB. Soil Viruses: A New Hope. *mSystems* 2019; 4: e00120-19.

772 7 Albright MBN, Gallegos-Graves LV, Feeser KL, Montoya K, Emerson JB, Shakya M *et al.*
773 Experimental evidence for the impact of soil viruses on carbon cycling during surface
774 plant litter decomposition. *ISME Communications* 2022; 2: 24.

775 8 Brum JR, Ignacio-Espinoza JC, Roux S, Doulcier G, Acinas SG, Alberti A *et al.* Patterns
776 and ecological drivers of ocean viral communities. *Science* 2015; 348: 1261498.

9 Wilhelm SW, Suttle CA. Viruses and Nutrient Cycles in the Sea. *BioScience* 1999; 49: 781–788.

10 Suttle CA. Viruses in the sea. Nature. 2005; 437: 356–361.

11 Roux S, Brum JR, Dutilh BE, Sunagawa S, Duhaime MB, Loy A *et al.* Ecogenomics and potential biogeochemical impacts of globally abundant ocean viruses. *Nature* 2016; 537: 689–693.

12 Weitz JS, Stock CA, Wilhelm SW, Bourouiba L, Coleman ML, Buchan A *et al.* A multitrophic model to quantify the effects of marine viruses on microbial food webs and ecosystem processes. *The ISME journal* 2015; 9: 1352–64.

13 Hurwitz BL, Hallam SJ, Sullivan MB. Metabolic reprogramming by viruses in the sunlit and dark ocean. *Genome Biology* 2013; 14: R123.

14 Trubl G, Solonenko N, Chittick L, Solonenko SA, Rich VI, Sullivan MB. Optimization of viral resuspension methods for carbon-rich soils along a permafrost thaw gradient. *PeerJ* 2016; 4: e1999.

15 Han L-L, Yu D-T, Zhang L-M, Shen J-P, He J-Z. Genetic and functional diversity of ubiquitous DNA viruses in selected Chinese agricultural soils. *Scientific reports* 2017; 7: 45142.

16 Ackermann H-W. Sad State of Phage Electron Microscopy. Please Shoot the Messenger. *Microorganisms* 2013; 2: 1–10.

17 Mortimore M. *Dryland Opportunities: A new paradigm for people, ecosystems and development*. IUCN, Gland, Switzerland, IIED, London, UK and UNDP, New York, USA: Nairobi, Kenya, 2009https://iied.org/sites/default/files/pdfs/migrate/G02572.pdf.

18 Birch HF. The effect of soil drying on humus decomposition and nitrogen availability. *Plant and Soil* 1958; 10: 9–31.

19 Barnard RL, Blazewicz SJ, Firestone MK. Rewetting of soil: Revisiting the origin of soil CO2 emissions. *Soil Biology and Biochemistry* 2020; 147: 107819.

803 20 Placella SA, Brodie EL, Firestone MK. Rainfall-induced carbon dioxide pulses result from
804 sequential resuscitation of phylogenetically clustered microbial groups. *Proceedings of*
805 *the National Academy of Sciences* 2012; 109: 10931–10936.
806 21 Blazewicz SJ, Schwartz E, Firestone MK. Growth and death of bacteria and fungi
807 underlie rainfall-induced carbon dioxide pulses from seasonally dried soil. *Ecology* 2014;
808 95: 1162–1172.
809 22 Fraser FC, Corstanje R, Deeks LK, Harris JA, Pawlett M, Todman LC *et al.* On the origin
810 of carbon dioxide released from rewetted soils. *Soil Biology and Biochemistry* 2016; 101:
811 1–5.
812 23 Blazewicz SJ, Hungate BA, Koch BJ, Nuccio EE, Morrissey E, Brodie EL *et al.* Taxon-
813 specific microbial growth and mortality patterns reveal distinct temporal population
814 responses to rewetting in a California grassland soil. *ISME Journal* 2020; 14: 1520–1532.
815 24 Williamson KE, Radosevich M, Smith DW, Wommack KE. Incidence of lysogeny within
816 temperate and extreme soil environments. *Environmental Microbiology* 2007; 9: 2563–
817 2574.
818 25 Weitz JS, Beckett SJ, Brum JR, Cael BB, Dushoff J. Lysis, lysogeny and virus–microbe
819 ratios. *Nature* 2017; 549: E1–E3.
820 26 Ghosh D, Roy K, Williamson KE, White DC, Wommack KE, Sublette KL *et al.* Prevalence
821 of lysogeny among soil bacteria and presence of 16S rRNA and trzN genes in viral-
822 community DNA. *Applied and environmental microbiology* 2008; 74: 495–502.
823 27 Nafissi N, Slavcev R. Bacteriophage recombination systems and biotechnical
824 applications. *Applied Microbiology and Biotechnology* 2014; 98: 2841–2851.
825 28 Correa AMS, Howard-Varona C, Coy SR, Buchan A, Sullivan MB, Weitz JS. Revisiting
826 the rules of life for viruses of microorganisms. *Nature Reviews Microbiology* 2021;
827 0123456789. doi:10.1038/s41579-021-00530-x.
828 29 Howard-Varona C, Hargreaves KR, Abedon ST, Sullivan MB. Lysogeny in nature:

829 mechanisms, impact and ecology of temperate phages. *The ISME Journal* 2017; 11:
830 1511–1520.
831 30 Ghosh D, Roy K, Williamson KE, Srinivasiah S, Wommack KE, Radosevich M. Acyl-
832 homoserine lactones can induce virus production in lysogenic bacteria: An alternative
833 paradigm for prophage induction. *Applied and Environmental Microbiology* 2009; 75:
834 7142–7152.
835 31 Brum JR, Hurwitz BL, Schofield O, Ducklow HW, Sullivan MB. Seasonal time bombs:
836 dominant temperate viruses affect Southern Ocean microbial dynamics. *The ISME*
837 *Journal* 2016; 10: 437–449.
838 32 Jurgensen SK, Roux S, Schwenck SM, Stewart FJ, Sullivan MB, Brum JR. Viral
839 community analysis in a marine oxygen minimum zone indicates increased potential for
840 viral manipulation of microbial physiological state. *The ISME Journal* 2022; 16: 972–982.
841 33 Schimel JP. Life in dry soils: Effects of drought on soil microbial communities and
842 processes. Annual Review of Ecology, Evolution, and Systematics. 2018; 49: 409–432.
843 34 Knowles B, Silveira CB, Bailey BA, Barott K, Cantu VA, Cobian-Guëmes AG *et al.* Lytic to
844 temperate switching of viral communities. *Nature* 2016; 531: 466–470.
845 35 Kimura M, Jia Z-J, Nakayama N, Asakawa S. Ecology of viruses in soils: Past, present
846 and future perspectives. *Soil Science and Plant Nutrition* 2008; 54: 1–32.
847 36 Wu R, Davison MR, Gao Y, Nicora CD, Mcdermott JE, Burnum-Johnson KE *et al.*
848 Moisture modulates soil reservoirs of active DNA and RNA viruses. *Communications*
849 *Biology* 2021; 4: 1–11.
850 37 Williamson KE, Radosevich M, Wommack KE. Abundance and diversity of viruses in six
851 Delaware soils. *Applied and Environmental Microbiology* 2005; 71: 3119–3125.
852 38 Placella SA, Firestone MK. Transcriptional response of nitrifying communities to wetting
853 of dry soil. *Applied and environmental microbiology* 2013; 79: 3294–302.
854 39 Barnard RL, Osborne CA, Firestone MK. Responses of soil bacterial and fungal

855 communities to extreme desiccation and rewetting. *The ISME Journal* 2013; 7: 2229–
856 2241.
857 40 Greenlon A, Sieradzki E, Zablocki O, Koch BJ, Foley MM, Kimbrel JA *et al.* Quantitative
858 Stable-Isotope Probing (qSIP) with Metagenomics Links Microbial Physiology and Activity
859 to Soil Moisture in Mediterranean-Climate Grassland Ecosystems. *mSystems* 2022; 7.
860 doi:10.1128/msystems.00417-22.
861 41 Nuccio EE, Blazewicz SJ, Lafler M, Campbell AN, Kakouridis A, Kimbrel JA *et al.* HT-SIP:
862 A semi-automated Stable Isotope Probing pipeline identifies interactions in the
863 hyphosphere of arbuscular mycorrhizal fungi. *bioRxiv* 2022.
864 doi:10.1101/2022.07.01.498377.
865 42 Lennon JT, Jones SE. Microbial seed banks: The ecological and evolutionary implications
866 of dormancy. Nature Reviews Microbiology. 2011; 9: 119–130.
867 43 Carini P, Marsden PJ, Leff JW, Morgan EE, Strickland MS, Fierer N. Relic DNA is
868 abundant in soil and obscures estimates of soil microbial diversity. *Nature Microbiology*
869 2016; 2: 16242.
870 44 Rousk J, Bååth E. Growth of saprotrophic fungi and bacteria in soil. *FEMS Microbiology*
871 *Ecology* 2011; 78: 17–30.
872 45 Couradeau E, Sasse J, Goudeau D, Nath N, Hazen TC, Bowen BP *et al.* Probing the
873 active fraction of soil microbiomes using BONCAT-FACS. *Nature Communications* 2019;
874 10: 2770.
875 46 Hungate BA, Mau RL, Schwartz E, Caporaso JG, Dijkstra P, van Gestel N *et al.*
876 Quantitative microbial ecology through stable isotope probing. *Applied and environmental*
877 *microbiology* 2015; 81: 7570–81.
878 47 Koch BJ, McHugh TA, Hayer M, Schwartz E, Blazewicz SJ, Dijkstra P *et al.* Estimating
879 taxon-specific population dynamics in diverse microbial communities. *Ecosphere* 2018; 9.
880 doi:10.1002/ecs2.2090.

881 48 Schwartz E. Characterization of growing microorganisms in soil by stable isotope probing
882 with H218O. *Applied and Environmental Microbiology* 2007; 73: 2541–2546.
883 49 Sieradzki ET, Greenlon A, Nicolas AM, Firestone MK, Pett-Ridge J, Blazewicz SJ *et al.*
884 Functional succession of actively growing soil microorganisms during rewetting is shaped
885 by precipitation history. *bioRxiv* 2022; : 2022.06.28.498032.
886 50 Nicolas AM, Jaffe AL, Nuccio EE, Taga ME, Firestone MK, Banfield JF. Soil Candidate
887 Phyla Radiation Bacteria Encode Components of Aerobic Metabolism and Co-occur with
888 Nanoarchaea in the Rare Biosphere of Rhizosphere Grassland Communities. *mSystems*
889 2021; 6. doi:10.1128/msystems.01205-20.
890 51 Thingstad TF. Elements of a theory for the mechanisms controlling abundance, diversity,
891 and biogeochemical role of lytic bacterial viruses in aquatic systems. *Limnology and*
892 *Oceanography* 2000; 45: 1320–1328.
893 52 Ignacio-Espinoza JC, Ahlgren NA, Fuhrman JA. Long-term stability and Red Queen-like
894 strain dynamics in marine viruses. *Nature Microbiology* 2020; 5: 265–271.
895 53 Cortez MH, Weitz JS. Coevolution can reverse predator–prey cycles. *Proceedings of the*
896 *National Academy of Sciences* 2014; 111: 7486–7491.
897 54 Chow C-ET, Kim DY, Sachdeva R, Caron DA, Fuhrman JA. Top-down controls on
898 bacterial community structure: microbial network analysis of bacteria, T4-like viruses and
899 protists. *The ISME Journal* 2014; 8: 816–829.
900 55 Kieft K, Anantharaman K. Deciphering Active Prophages from Metagenomes. *mSystems*
901 2022. doi:10.1128/msystems.00084-22.
902 56 Roux S, Krupovic M, Daly RA, Borges AL, Nayfach S, Schulz F *et al.* Cryptic inoviruses
903 revealed as pervasive in bacteria and archaea across Earth's biomes. *Nature*
904 *Microbiology* 2019; 4: 1895–1906.
905 57 Williamson KE, Schnitker JB, Radosevich M, Smith DW, Wommack KE. Cultivation-
906 based assessment of lysogeny among soil bacteria. *Microbial ecology* 2008; 56: 437–47.

58 Sui B, Qi X, Wang X, Ren H, Liu W, Zhang C. Characterization of a Novel Bacteriophage swi2 Harboring Two Lysins Can Naturally Lyse Escherichia coli. *Frontiers in Microbiology* 2021; 12: 1201.

59 Orgiazzi A, Bardgett RD, Barrios E, Behan-Pelletier V, Briones MJI, Chotte J-L *et al.* (eds.). *Global Soil Biodiversity Atlas*. European Commission, 2016 doi:10.2788/2613.

60 Sokol NW, Slessarev E, Marschmann GL, Nicolas A, Blazewicz SJ, Brodie EL *et al.* Life and death in the soil microbiome: how ecological processes influence biogeochemistry. *Nature Reviews Microbiology* 2022; 0123456789. doi:10.1038/s41579-022-00695-z.

61 Yan Y, Klinkhamer PGL, van Veen JA, Kuramae EE. Environmental filtering: A case of bacterial community assembly in soil. *Soil Biology and Biochemistry* 2019; 136: 107531.

62 Romdhane S, Spor A, Aubert J, Bru D, Breuil MC, Hallin S *et al.* Unraveling negative biotic interactions determining soil microbial community assembly and functioning. *ISME Journal* 2022; 16: 296–306.

63 Zegeye EK, Brislawn CJ, Farris Y, Fansler SJ, Hofmockel KS, Jansson JK *et al.* Selection, Succession, and Stabilization of Soil Microbial Consortia. *mSystems* 2019; 4: 55–74.

64 Nemergut DR, Schmidt SK, Fukami T, O'Neill SP, Bilinski TM, Stanish LF *et al.* Patterns and Processes of Microbial Community Assembly. *Microbiology and Molecular Biology Reviews* 2013; 77: 342–356.

65 Wang C, Michalet R, Liu Z, Jiang X, Wang X, Zhang G *et al.* Disentangling Large- and Small-Scale Abiotic and Biotic Factors Shaping Soil Microbial Communities in an Alpine Cushion Plant System. *Frontiers in Microbiology* 2020; 11: 925.

66 Wilpiszeski RL, Aufrecht JA, Retterer ST, Sullivan MB, Graham DE, Pierce EM *et al.* Soil Aggregate Microbial Communities: Towards Understanding Microbiome Interactions at Biologically Relevant Scales. Applied and environmental microbiology. 2019; 85. doi:10.1128/AEM.00324-19.

933 67 Jansson JK, Hofmockel KS. Soil microbiomes and climate change. Nature Reviews
934 Microbiology. 2020; 18: 35–46.
935 68 Miller R V., Day MJ. Contribution of lysogeny, pseudolysogeny, and starvation to phage
936 ecology. In: Abedon ST (ed). *Bacteriophage Ecology*. Cambridge University Press:
937 Cambridge, 2009, pp 114–144.
938 69 Naylor D, Sadler N, Bhattacharjee A, Graham EB, Anderton CR, McClure R *et al.* Soil
939 microbiomes under climate change and implications for carbon cycling. Annual Review of
940 Environment and Resources. 2020; 45: 29–59.
941 70 Jover LF, Effler TC, Buchan A, Wilhelm SW, Weitz JS. The elemental composition of
942 virus particles: Implications for marine biogeochemical cycles. *Nature Reviews*
943 *Microbiology* 2014; 12: 519–528.
944 71 Suttle CA. The significance of viruses to mortality in aquatic microbial communities.
945 *Microbial Ecology* 1994; 28: 237–243.
946 72 Starr EP, Shi S, Blazewicz SJ, Koch BJ, Probst AJ, Hungate BA *et al.* Stable-Isotope-
947 Informed, Genome-Resolved Metagenomics Uncovers Potential Cross-Kingdom
948 Interactions in Rhizosphere Soil. *mSphere* 2021; 6. doi:10.1128/mSphere.00085-21.
949 73 Pett-Ridge J, Firestone MK. Using stable isotopes to explore root-microbe-mineral
950 interactions in soil. *Rhizosphere* 2017. doi:10.1016/j.rhisph.2017.04.016.
951 74 Tecon R, Ebrahimi A, Kleyer H, Erev Levi S, Or D. Cell-to-cell bacterial interactions
952 promoted by drier conditions on soil surfaces. *Proceedings of the National Academy of*
953 *Sciences of the United States of America* 2018; 115: 9791–9796.
954 75 Jiao S, Yang Y, Xu Y, Zhang J, Lu Y. Balance between community assembly processes
955 mediates species coexistence in agricultural soil microbiomes across eastern China. *The*
956 *ISME Journal* 2020; 14: 202–216.
957 76 Durham DM, Sieradzki ET, ter Horst AM, Santos-Medellín C, Bess CWA, Geonczy SE *et*
958 *al.* Substantial differences in soil viral community composition within and among four

959 Northern California habitats. *ISME Communications* 2022; 2: 100.
960 77 Santos-Medellín C, Estera-Molina K, Yuan M, Pett-Ridge J, Firestone MK, Emerson JB.
961 Spatial turnover of soil viral populations and genotypes overlain by cohesive responses to
962 moisture in grasslands. *Proceedings of the National Academy of Sciences* 2022; 119: 1–
963 11.
964 78 Burstein D, Sun CL, Brown CT, Sharon I, Anantharaman K, Probst AJ *et al.* Major
965 bacterial lineages are essentially devoid of CRISPR-Cas viral defence systems. *Nature*
966 *Communications* 2016; 7: 10613.
967 79 Joshi N, Fass J. Sickle: A sliding-window, adaptive, quality-based trimming tool for FastQ
968 files (Version 1.33). 2011.
969 80 Li D, Liu C-M, Luo R, Sadakane K, Lam T-W. MEGAHIT: an ultra-fast single-node
970 solution for large and complex metagenomics assembly via succinct de Bruijn graph.
971 *Bioinformatics* 2015; 31: 1674–1676.
972 81 Hyatt D, Chen G-L, Locascio PF, Land ML, Larimer FW, Hauser LJ. Prodigal: prokaryotic
973 gene recognition and translation initiation site identification. *BMC bioinformatics* 2010; 11:
974 119.
975 82 Edgar RC. Search and clustering orders of magnitude faster than BLAST. *Bioinformatics*
976 2010; 26: 2460–2461.
977 83 Ogata H, Goto S, Sato K, Fujibuchi W, Bono H, Kanehisa M. KEGG: Kyoto encyclopedia
978 of genes and genomes. Nucleic Acids Research. 1999; 27: 29–34.
979 84 Suzek BE, Huang H, McGarvey P, Mazumder R, Wu CH. UniRef: comprehensive and
980 non-redundant UniProt reference clusters. *Bioinformatics* 2007; 23: 1282–1288.
981 85 Magrane M, UniProt Consortium. UniProt Knowledgebase: A hub of integrated protein
982 data. *Database* 2011; 2011. doi:10.1093/database/bar009.
983 86 Wu Y-W, Tang Y-H, Tringe SG, Simmons BA, Singer SW. MaxBin: an automated binning
984 method to recover individual genomes from metagenomes using an expectation-

985 maximization algorithm. *Microbiome* 2014; 2: 26.
986 87 Kang DD, Froula J, Egan R, Wang Z. MetaBAT, an efficient tool for accurately
987 reconstructing single genomes from complex microbial communities. *PeerJ* 2015; 3:
988 e1165.
989 88 Alneberg J, Bjarnason BS, De Bruijn I, Schirmer M, Quick J, Ijaz UZ *et al.* Binning
990 metagenomic contigs by coverage and composition. *Nature Methods* 2014; 11: 1144–
991 1146.
992 89 Sieber CMK, Probst AJ, Sharrar A, Thomas BC, Hess M, Tringe SG *et al.* Recovery of
993 genomes from metagenomes via a dereplication, aggregation and scoring strategy.
994 *Nature Microbiology* 2018; 3: 836–843.
995 90 Olm MR, Brown CT, Brooks B, Banfield JF. dRep: a tool for fast and accurate genomic
996 comparisons that enables improved genome recovery from metagenomes through de-
997 replication. *The ISME Journal* 2017; 11: 2864–2868.
998 91 Roux S, Enault F, Hurwitz BL, Sullivan MB. VirSorter: mining viral signal from microbial
999 genomic data. *PeerJ* 2015; 3: e985.
1000 92 Guo J, Bolduc B, Zayed AA, Varsani A, Dominguez-Huerta G, Delmont TO *et al.*
1001 VirSorter2: a multi-classifier, expert-guided approach to detect diverse DNA and RNA
1002 viruses. *Microbiome* 2021; 9: 37.
1003 93 Kieft K, Zhou Z, Anantharaman K. VIBRANT: Automated recovery, annotation and
1004 curation of microbial viruses, and evaluation of viral community function from genomic
1005 sequences. *Microbiome* 2020; 8: 90.
1006 94 Ren J, Song K, Deng C, Ahlgren NA, Fuhrman JA, Li Y *et al.* Identifying viruses from
1007 metagenomic data using deep learning. *Quantitative Biology* 2020; 8: 64–77.
1008 95 Auslander N, Gussow AB, Benler S, Wolf YI, Koonin E V. Seeker: Alignment-free
1009 identification of bacteriophage genomes by deep learning. *Nucleic Acids Research* 2020;
1010 48: E121.

1011 96 Crits-Christoph A, Gelsinger DR, Ma B, Wierzchos J, Ravel J, Davila A *et al.* Functional
1012 interactions of archaea, bacteria and viruses in a hypersaline endolithic community.
1013 *Environmental microbiology* 2016; 18: 2064–2077.
1014 97 Shaffer M, Borton MA, McGivern BB, Zayed AA, La Rosa SL 0003 3527 8101, Solden LM
1015 *et al.* DRAM for distilling microbial metabolism to automate the curation of microbiome
1016 function. *Nucleic Acids Research* 2020; 48: 8883–8900.
1017 98 Barnard RL, Osborne CA, Firestone MK. Changing precipitation pattern alters soil
1018 microbial community response to wet-up under a Mediterranean-type climate. *The ISME*
1019 *Journal* 2015; 9: 946–957.
1020 99 Uritskiy G V., Diruggiero J, Taylor J. MetaWRAP - A flexible pipeline for genome-resolved
1021 metagenomic data analysis 08 Information and Computing Sciences 0803 Computer
1022 Software 08 Information and Computing Sciences 0806 Information Systems. *Microbiome*
1023 2018; 6. doi:10.1186/s40168-018-0541-1.
1024 100 Chaumeil PA, Mussig AJ, Hugenholtz P, Parks DH. GTDB-Tk: A toolkit to classify
1025 genomes with the genome taxonomy database. *Bioinformatics* 2020; 36: 1925–1927.
1026 101 Li H, Handsaker B, Wysoker A, Fennell T, Ruan J, Homer N *et al.* The Sequence
1027 Alignment/Map format and SAMtools. *Bioinformatics* 2009; 25: 2078–2079.
1028 102 Virtanen P, Gommers R, Oliphant TE, Haberland M, Reddy T, Cournapeau D *et al.* SciPy
1029 1.0: fundamental algorithms for scientific computing in Python. *Nature Methods* 2020; 17:
1030 261–272.
1031 103 Bland C, Ramsey TL, Sabree F, Lowe M, Brown K, Kyrpides NC *et al.* CRISPR
1032 Recognition Tool (CRT): A tool for automatic detection of clustered regularly interspaced
1033 palindromic repeats. *BMC Bioinformatics* 2007; 8: 209.
1034 104 Altschul SF, Gish W, Miller W, Myers EW, Lipman DJ. Basic local alignment search tool.
1035 *Journal of Molecular Biology* 1990; 215: 403–410.
1036 105 Menzel P, Ng KL, Krogh A. Fast and sensitive taxonomic classification for metagenomics

1037 with Kaiju. *Nature Communications* 2016; 7. doi:10.1038/ncomms11257.
1038 106 Shmakov SA, Sitnik V, Makarova KS, Wolf YI, Severinov K V, Koonin E V. The CRISPR
1039 Spacer Space Is Dominated by Sequences from Species-Specific Mobilomes. *mBio*
1040 2017; 8: e01397-17.
1041 107 Al-Shayeb B, Sachdeva R, Chen LX, Ward F, Munk P, Devoto A *et al.* Clades of huge
1042 phages from across Earth's ecosystems. *Nature* 2020; 578: 425–431.
1043 108 Mihara T, Nishimura Y, Shimizu Y, Nishiyama H, Yoshikawa G, Uehara H *et al.* Linking
1044 Virus Genomes with Host Taxonomy. *Viruses* 2016; 8: 66.
1045 109 Waskom M. seaborn: statistical data visualization. *Journal of Open Source Software*
1046 2021; 6: 3021.
1047 110 Klappenbach JA, Dunbar JM, Schmidt TM. rRNA operon copy number reflects ecological
1048 strategies of bacteria. *Applied and Environmental Microbiology* 2000; 66: 1328–1333.
1049
1050

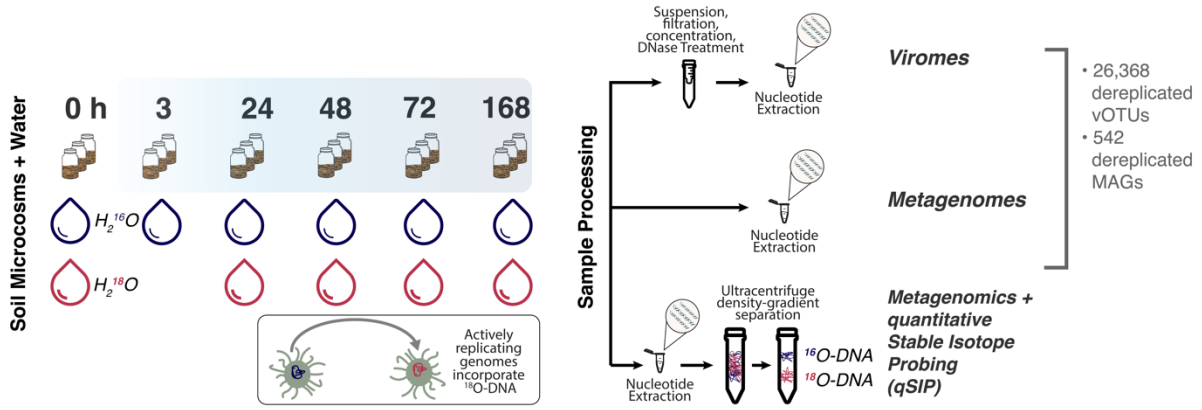

Figure 1 | Experimental overview describing recovery of genomes from time-resolved cellular (metagenomes) and viral size-fraction metagenomes (viromes) following soil wet-up. Triplicate sampled soil microcosms were destructively harvested before (0 h) or following addition of natural abundance water ($H_2{}^{16}O$) (3 h, 24 h, 48 h, 72 and 168 h) for the generation of viromes and metagenomes or with $H_2{}^{18}O$, stable isotope-enriched water, for metagenomics with quantitative stable isotope probing (qSIP). Below the depiction of the microcosms is a cartoon of a microbial cell and its genome before (blue) and after (red) incorporation of ^{18}O-DNA. Microcosms fated for metagenomic sequencing did not include a 3h time point. Sample prep for viromes, metagenomes, and qSIP metagenomics prior to shotgun sequencing is shown on the right.

1051

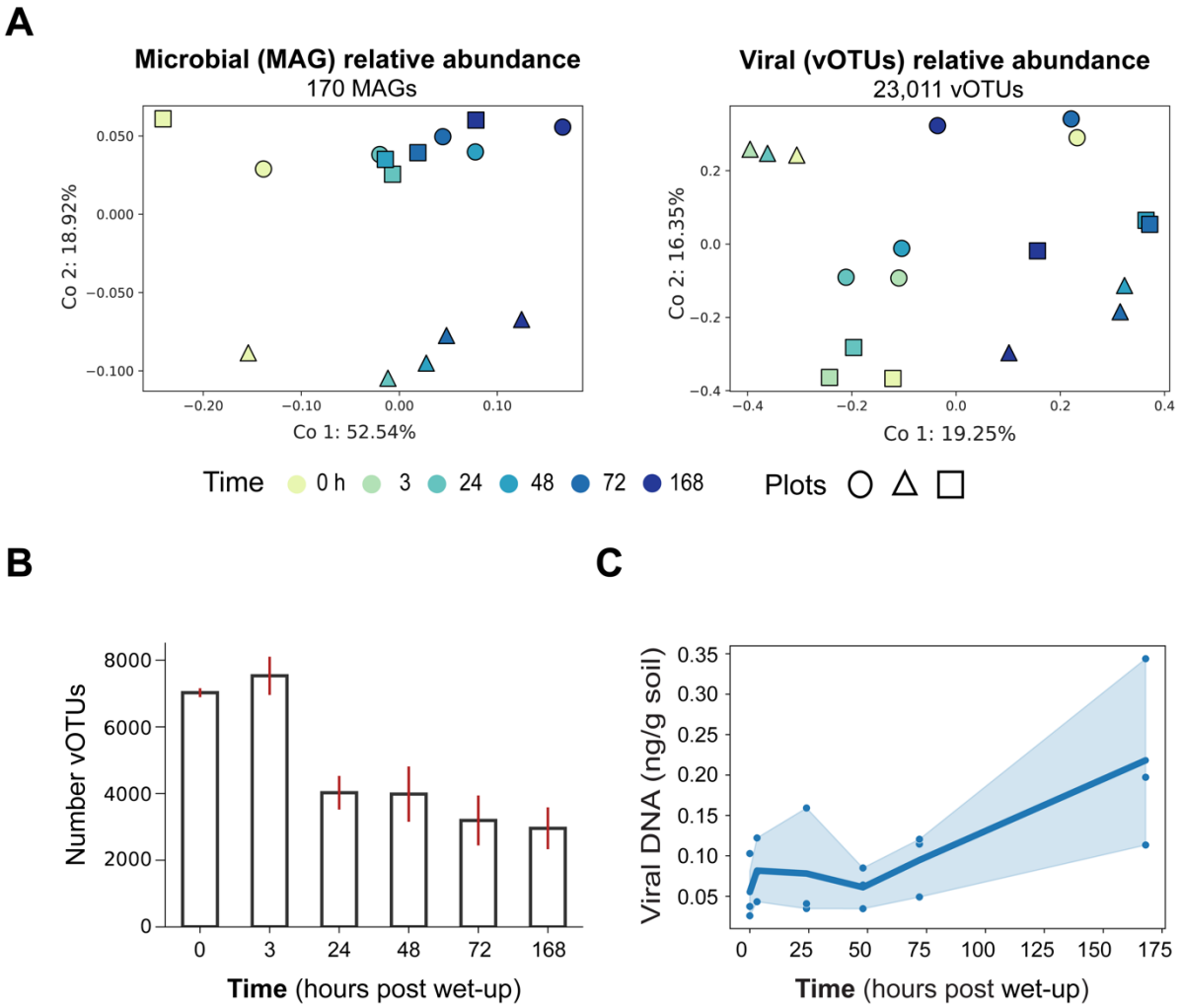

Figure 2 | Temporal compositional changes in microbial and viral communities following soil wet-up. **(A)** PCoA plots of MAGs (left) and vOTUs (right) calculated based on Bray-Curtis dissimilarity colored by time with different marker shapes signifying distinct field plots (biological replicates). **(B)** Barplot of the mean total number of unique vOTUs per time point. Error bars (red) show standard error of mean across all three field plots. **(C)** Viral biomass approximated by total extracted viral DNA (ng) per gram of soil plotted through time. Each point represents a distinct microcosm. The shaded area around the line represents a 95% confidence interval.

1052

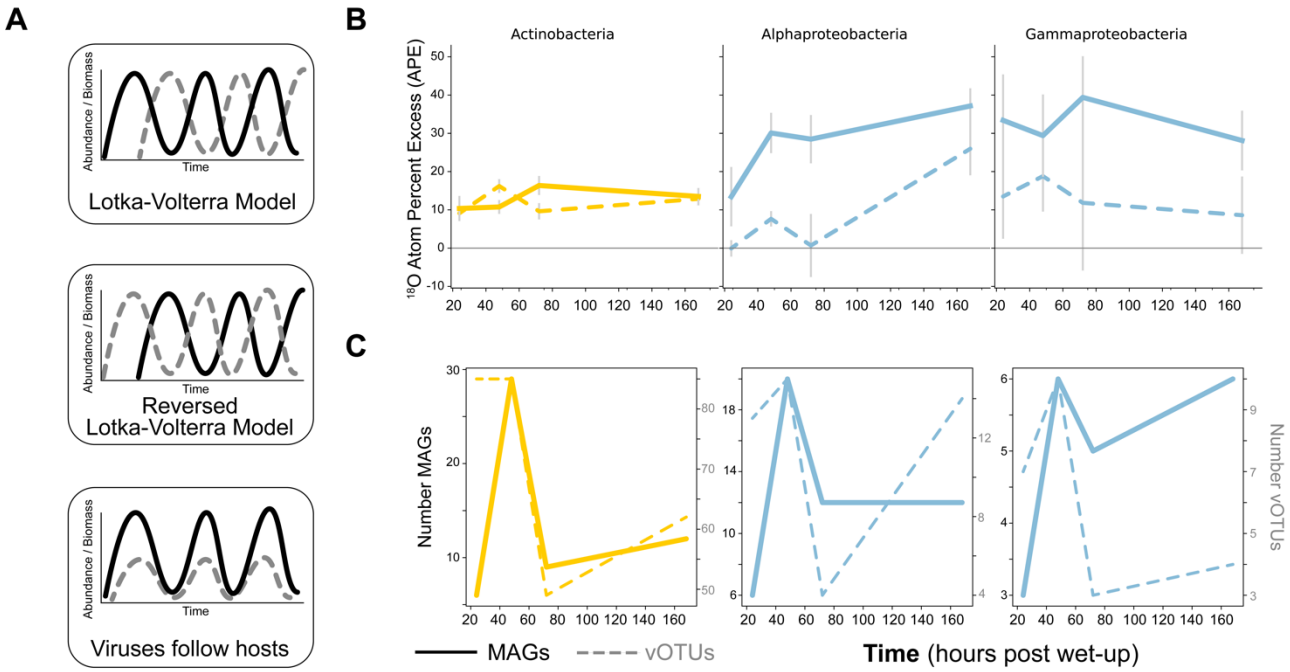

Figure 3 | Dynamics of isotope-enriched (growing) viruses and microbes through time following soil wet-up. Viruses or vOTUs are represented in all plots by dotted line, MAGs are depicted by solid line. Colors represent taxonomic groups (yellow are Actinobacteria, blue are Proteobacteria). **(A)** Hypothetical models of viral predation on microbes: Lotka-Volterra model, reversed Lotka-Volterra, and a model in which viruses track changes in host abundance. **(B)** Mean ^{18}O atom percent excess (APE) for MAGs and vOTUs through time post wet-up. Error bars represent standard error of genome APE means. **(C)** Number of unique MAGs and vOTUs per lineage detected as incorporating isotope at each time point post wet-up.

1053

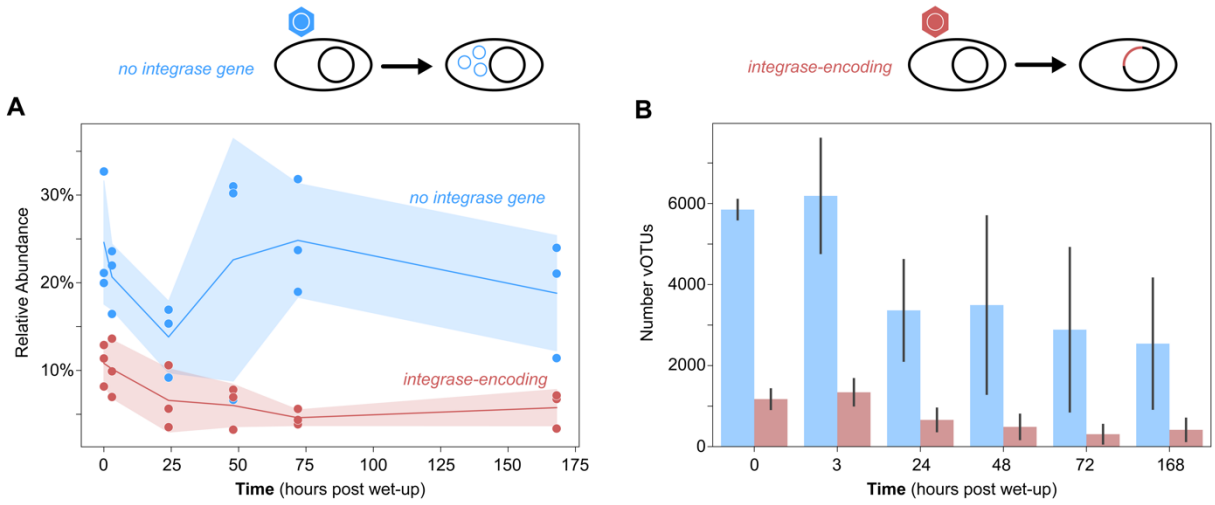

Figure 4 | Relative abundance and richness of integrase-encoding vOTUs through time following soil wet-up. vOTUs were split by whether they encode an integrase gene (red) or not (blue). Cartoon above illustrates integrase-encoding vOTUs (red hexagon) have the capacity for their genomes to integrate into their host's chromosome or no integrase gene vOTUs (blue hexagon) may not be able to integrate their genome into a host's genome. **(A)** Relative abundance (percent of total sampled reads) of integrase-encoding or not integrase-encoding vOTUs. **(B)** Counts of integrase-containing and non-integrase containing vOTUs.

1054

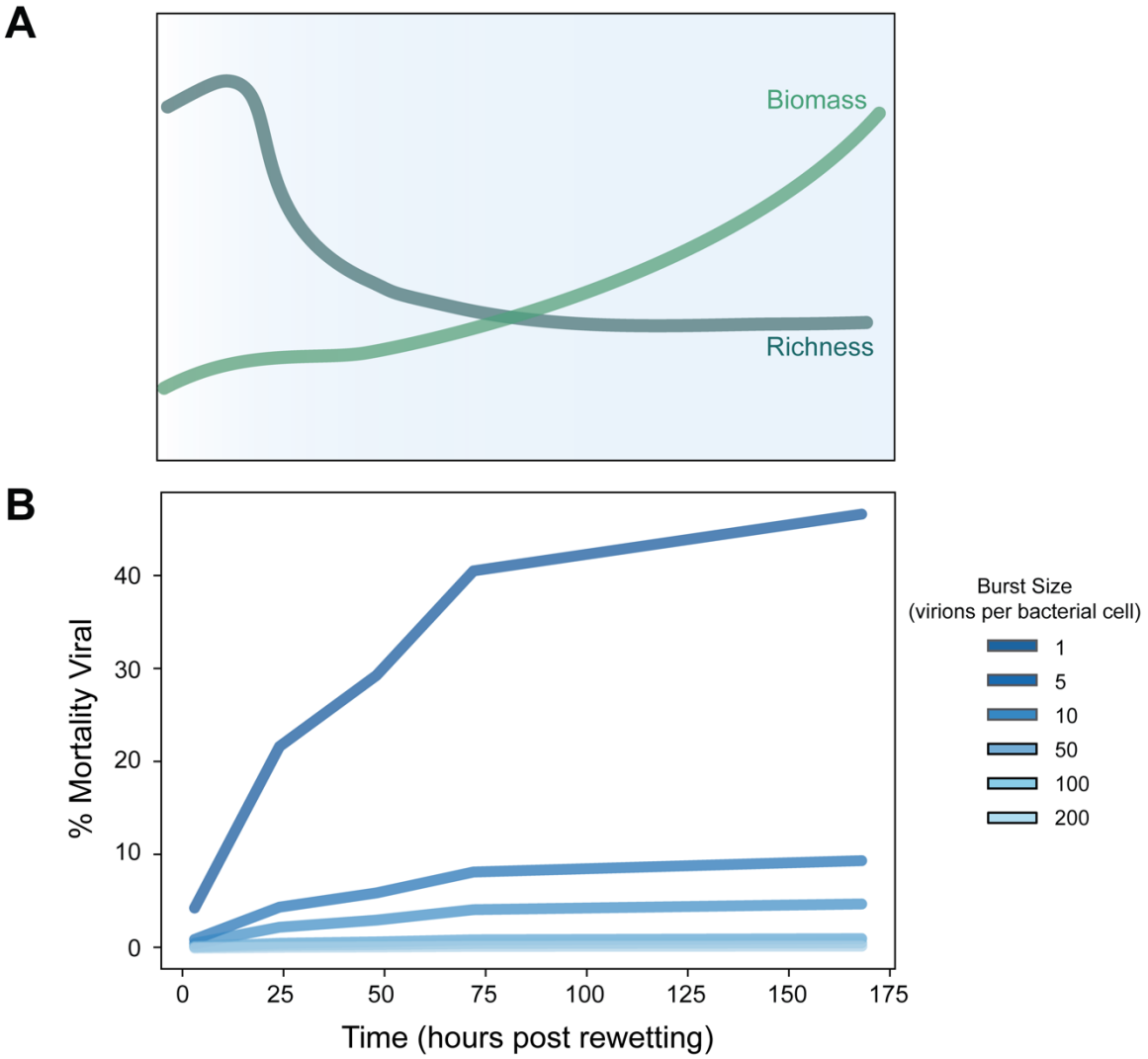

Figure 5 | Viral response to wet-up and corresponding contribution to microbial mortality. **(A)** Conceptual model of changes in viral richness (gray-blue) and biomass (green) over time. **(B)** Modelled contribution of viruses to microbial mortality where each line graphed represents an estimated percent contribution for a different viral burst size shown in the legend ranging from 1 virion per lysed microbial cell to 1000 virions per lysed microbial cell.

1055